Human Molecular Genetics, 2010, Vol. 19, No. 7 ***1335–1346***
doi:10.1093/hmg/ddq010
Advance Access published on January 20, 2010

α-Actinin-3 deficiency results in reduced glycogen phosphorylase activity and altered calcium handling in skeletal muscle

Kate G.R. Quinlan[1,2], Jane T. Seto[1,2], Nigel Turner[3,4], Aurelie Vandebrouck[1], Matthias Floetenmeyer[5], Daniel G. Macarthur[1], Joanna M. Raftery[1], Monkol Lek[1,2], Nan Yang[1,2], Robert G. Parton[5,6], Gregory J. Cooney[3,4] and Kathryn N. North[1,2,*]

[1]Institute for Neuroscience and Muscle Research, The Children's Hospital at Westmead, Sydney, NSW 2145, Australia, [2]Discipline of Paediatrics and Child Health, Faculty of Medicine, University of Sydney, Sydney, NSW 2006, Australia, [3]Diabetes and Obesity Program, Garvan Institute of Medical Research, Darlinghurst, NSW 2010, Australia, [4]St Vincent's Hospital Clinical School, University of New South Wales, Sydney, NSW 2010, Australia, [5]Centre for Microscopy and Microanalysis, The University of Queensland, St Lucia, QLD 4072, Australia and [6]Institute for Molecular Bioscience, The University of Queensland, St Lucia, QLD 4072, Australia

Received September 25, 2009; Revised December 23, 2009; Accepted January 11, 2010

Approximately one billion people worldwide are homozygous for a stop codon polymorphism in the *ACTN3* gene (R577X) which results in complete deficiency of the fast fibre muscle protein α-actinin-3. *ACTN3* genotype is associated with human athletic performance and α-actinin-3 deficient mice [*Actn3* knockout (KO) mice] have a shift in the properties of fast muscle fibres towards slower fibre properties, with increased activity of multiple enzymes in the aerobic metabolic pathway and slower contractile properties. α-Actinins have been shown to interact with a number of muscle proteins including the key metabolic regulator glycogen phosphorylase (GPh). In this study, we demonstrated a link between α-actinin-3 and glycogen metabolism which may underlie the metabolic changes seen in the KO mouse. *Actn3* KO mice have higher muscle glycogen content and a 50% reduction in the activity of GPh. The reduction in enzyme activity is accompanied by altered post-translational modification of GPh, suggesting that α-actinin-3 regulates GPh activity by altering its level of phosphorylation. We propose that the changes in glycogen metabolism underlie the downstream metabolic consequences of α-actinin-3 deficiency. Finally, as GPh has been shown to regulate calcium handling, we examined calcium handling in KO mouse primary mouse myoblasts and find changes that may explain the slower contractile properties previously observed in these mice. We propose that the alteration in GPh activity in the absence of α-actinin-3 is a fundamental mechanistic link in the association between *ACTN3* genotype and human performance.

INTRODUCTION

α-Actinin-3 is a structural fast skeletal muscle protein encoded by the *ACTN3* gene (1). A common polymorphism in this gene, R577X, results in a premature stop codon in the place of an arginine residue at position 577. Individuals with two copies of the X allele (*ACTN3* 577XX genotype) are completely deficient in α-actinin-3 (2). Although 577XX genotype frequencies differ between human populations, it is estimated that 16% of individuals worldwide, or approximately one billion people, are deficient in α-actinin-3 (3). Hence understanding the consequences of α-actinin-3 deficiency in humans may have wide-reaching implications.

ACTN3 genotype has been linked with elite athletic performance in humans. The 577XX genotype is underrepresented in Australian Caucasian sprint athletes and slightly over-represented in endurance athletes compared with non-athlete controls (4). This association has been independently

*To whom correspondence should be addressed. Tel: +61 298451906; Fax: +61 298453389; Email: kathryn@chw.edu.au

replicated in six European, Israeli and North American athlete cohorts (5–10). The 577XX genotype is also associated with muscle performance in non-athletes; 577XX women demonstrated significantly lower voluntary elbow contraction force than 577RR women (11) and 577XX Greek adolescent boys recorded significantly slower 40 m sprint times than 577RR individuals (12). In combination, these data provide strong evidence that α-actinin-3 deficiency is detrimental to sprint and power performance. The expression of α-actinin-3 is restricted to fast type 2 muscle fibres in mouse and humans (3,13) suggesting that it plays a specific role in these muscle fibres which are responsible for forceful and rapid contraction. We have previously shown that the region around the R577X polymorphism bears low genetic variation and recombination, suggestive of positive selection on the X allele during recent human evolution (14).

We have generated a knockout (KO) mouse model in order to analyse the effects of α-actinin-3 deficiency on skeletal muscle function (14). 'Fast' muscles in the KO mice display slower muscle properties, including slower contractile properties, providing a potential explanation for the low frequency of α-actinin-3 deficiency among sprint athletes. Interestingly, KO mice displayed a number of metabolic differences to wild-type (WT) littermates, with increases in the maximal activity of key enzymes of glycolysis and aerobic metabolism, but decreases in maximal activity of an anaerobic metabolism enzyme (15). These metabolic differences may underlie the selective advantage of the 577X allele during recent human evolution, possibly through increased metabolic 'thriftiness' or improved cold tolerance (14).

α-Actinin-3 and the highly homologous protein α-actinin-2 cross-link actin and are major protein components of the Z-line in the skeletal muscle contractile apparatus. The mammalian sarcomeric α-actinins, α-actinin-2 and -3 have been shown to interact with a large number of structural muscle proteins in addition to actin including myotilin (16), dystrophin (17), actin-associated LIM protein (18,19), nebulin-related anchoring protein (20), enigma homologue (21), titin (22) and Z-band alternatively spliced PDZ motif (23). Thus, α-actinin-2 and -3 are considered to be structural muscle proteins. The majority of these interactions have been demonstrated using either α-actinin-2 or purified α-actinin from muscle (a mixture of α-actinin-2 and -3); however, due to the high sequence homology within the α-actinins, many interactions are likely to also occur with α-actinin-3. Binding partners such as the signalling proteins calsarcin 1, 2 and 3 (24) and protein kinase N (25), voltage gated ion channels Kv1.4 and Kv1.5 (26,27) and metabolic enzymes glycogen phosphorylase (GPh) (28) and fructose-1,6-bisphosphatase (29) suggest additional roles for the sarcomeric α-actinins beyond their characterized structural role.

Fast muscle fibres in which α-actinin-3 is normally expressed are particularly reliant on mobilization of intracellular glycogen stores to provide the energy required for contraction. A change in the ability of the muscle to utilize glycogen as an energy source could be expected to alter the metabolic state of the muscle as the cells strive to produce energy using alternate pathways. We have previously shown that our KO mice have increased marker enzyme activities for the glycolysis and aerobic metabolism pathways but decreased anaerobic metabolism. We hypothesized that the reported interaction of α-actinins with GPh (28) could relate to the metabolic effects seen in the KO mice—a hypothesis that we aimed to test in this study. We demonstrate that there is increased glycogen content in KO muscle and that GPh activity is reduced in KO muscle but that this is not associated with a gross alteration in the localization of GPh. We detect cytoplasmic inclusions in KO muscles which contain GPh. We also show that GPh co-localizes with α-actinin-3 at the Z-line in skeletal muscle. To strengthen the link between α-actinin-3 deficiency and lower activity of GPh, we demonstrate that the post-translational modifications of GPh are altered in KO muscle. The onset of glycogen metabolism perturbation occurs concomitantly with the increased glycolysis and aerobic metabolism during post-natal development suggesting that these consequences of α-actinin-3 deficiency may be linked. Finally, due to a previously reported association between GPh activity and calcium release, we test calcium handling in primary mouse myoblast cultures from WT and KO mice and show that calcium handling is altered. Our data support a role for α-actinin-3 in the regulation of the phosphorylation of GPh and suggest that alterations in GPh activity in the absence of α-actinin-3 underlie the metabolic and contractile changes seen in KO mouse muscle.

RESULTS

Glycogen content is higher in α-actinin-3 deficient muscles

We initially hypothesized that glycogen metabolism is altered in α-actinin-3 deficient muscle, based on the known interaction between the sarcomeric α-actinins and GPh (28). To test this hypothesis, we examined the glycogen content of WT and KO mouse muscles by periodic acid-Schiff (PAS) staining. PAS staining was visibly more intense in KO muscle sections than WT, indicating higher glycogen content (Fig. 1A), and quantitative pixel intensity was significantly higher in KO than WT muscle (data not shown). To quantitate glycogen content more precisely, glycogen assays were performed on a range of KO and WT muscles (Fig. 1B). Glycogen content was significantly higher in KO tibialis anterior, gastrocnemius, quadriceps and spinalis muscles. The extensor digitorum longus muscle showed a trend towards higher glycogen content but this did not reach significance. No differences in glycogen content were seen between WT and KO mice in the soleus muscle, a slow muscle with very few of the fast-type 2B fibres in which α-actinin-3 is normally expressed, or in the heart (data not shown) where α-actinin-3 is not expressed. This suggests that the higher glycogen content in KO mice is a specific effect of α-actinin-3 deficiency. To further examine the glycogen content, we performed dual axis electron microscopic tomography on 300 nm thick sections of KO and WT samples. Glycogen was readily visualized in the tomograms and an estimate of glycogen content was obtained by quantitation of glycogen on multiple planes of the tomogram (Supplementary Material, Fig. S1). Glycogen volume as a percentage of the cytoplasmic volume was ∼1.9% in KO as opposed to ∼1.0% in WT mice. Taken together, these three lines of evidence strongly suggest that glycogen content is higher in KO than WT muscles.

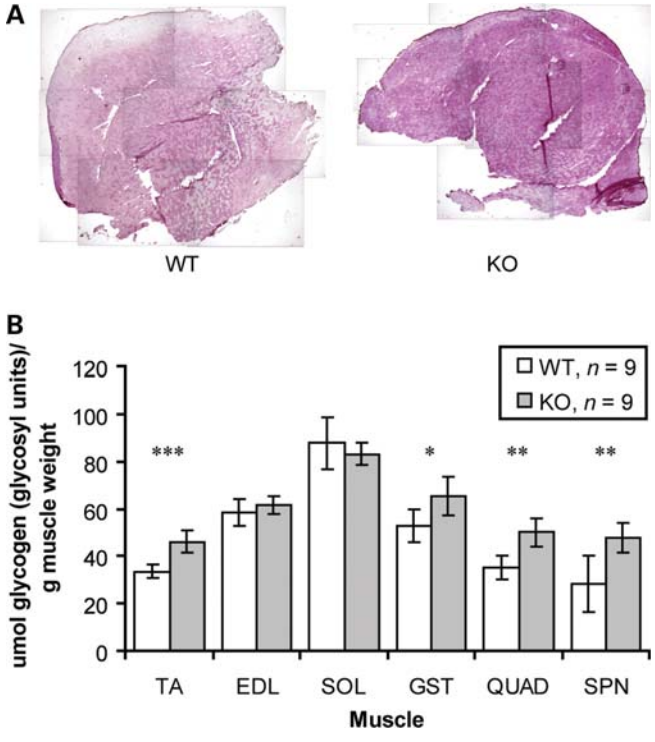

Figure 1. *Actn3* KO mice have more muscle glycogen. (**A**) Representative PAS staining images of 8-week-old male mouse quadriceps muscle cross-sections demonstrate that glycogen levels are higher in KO than WT muscle. (**B**) Glycogen assays on lower hind leg muscles tibialis anterior (TA), extensor digitorum longus (EDL), soleus (SOL) and gastrocnemius (GST), the upper hind leg muscle, quadriceps (QUAD) and the back muscle spinalis thoracis (SPN) from 8-week-old female WT ($n = 9$) and KO ($n = 9$) mice. Mean $\pm$ 95% CI, $^{*}P < 0.05$, $^{**}P < 0.01$, $^{***}P < 0.001$.

To determine whether glycogen content is altered in α-actinin-3 deficient humans, we performed glycogen content assays on human quadriceps muscle samples. The human muscle was obtained from people undergoing testing for malignant hyperthermia and the muscle used was from those who tested negative on all tests. The human cohort contained 26 individuals, of which 10 were males and 16 were females, with 9 of *ACTN3* 577RR genotype, 12 of 577RX genotype and 5 of 577XX genotype. The age range for the individuals was 11–67 years at date of biopsy with mean age of 40.1 years and median age of 37.2 years. No biometric data or information on the exercise status of these individuals was available. The glycogen content was significantly higher in the 577XX individuals than in the 577RX individuals and there was a trend towards higher glycogen content in the 577XX individuals compared with the 577RR individuals (Supplementary Material, Fig. S2). These results suggest that the higher muscle glycogen content observed in α-actinin-3 deficient mice also occurs in α-actinin-3 deficient humans.

Glycogen phosphorylase activity is lower in muscles in the absence of α-actinin-3

The differences in glycogen content seen in our KO mice could result from either an increase in the level or activity of the key regulatory enzyme of glycogen synthesis, glycogen synthase (GS), or a decrease in the levels or activity of the key regulatory enzyme of glycogen degradation, GPh, or in phosphorylase kinase (PK) which phosphorylates and activates GPh (Fig. 2A).

There were no differences in the total expression levels of GS, GPh or PK in WT and KO muscle by western blot (Fig. 2B). However, both GS and GPh are regulated by reversible phosphorylation and, as such, the activity of these enzymes can vary without any change in the total levels. We assayed GS and GPh activity in WT and KO muscle both in the absence and presence of allosteric activators of these enzymes, glucose-6-phosphate and AMP, respectively. The activity measurement of each enzyme in the absence of the allosteric activator allows the level of the enzyme that is active to be determined. This value can be compared with the activity measurement in the presence of the allosteric activator, which stimulates the inactive portion of the enzyme into activity and hence allows the total enzyme level to be assessed. While we saw significantly higher levels of both active and total GS in the KO muscles, there was no significant difference in the percentage activity of this enzyme between the WT and KO mice (Fig. 2C). The lack of differences in the percentage activity suggests that the regulation of GS activity is not altered by the absence of α-actinin-3. However, the increase in the total level of GS seen in the mouse muscle could contribute to the increased glycogen content seen in KO mice.

The level of active GPh and the percentage activity of GPh was significantly lower in the KO (26%) when compared with 53% in the WT mice, whereas the total amount of the enzyme was unchanged (Fig. 2C). This suggests that the regulation of GPh activity is altered in muscle in the absence of α-actinin-3. Such a large decrease in the activity of GPh (~50% of WT) would be predicted to reduce the ability of muscle to degrade glycogen, and likely contributes substantially to the increased glycogen content in KO muscle.

To determine whether the GPh activity was altered in α-actinin-3 deficient humans, muscle from the cohort of 26 individuals described earlier was examined for GPh activity. There was a trend towards an increase in total GPh and for a decreased GPh % activity in the 577XX (α-actinin-3 deficient) group when compared with the RR or RX groups (Supplementary Material, Fig. S2). Due to the inherent variability in human samples and the small number of individuals in our human cohort, a larger group of age, gender and exercise status matched individuals would be required to investigate the relationship between α-actinin-3 and GPh activity in humans conclusively.

Glycogen phosphorylase forms cytoplasmic inclusions in KO muscle

Next we examined the expression of GPh in WT and KO muscle by immunohistochemistry (IHC). In cross-sectional muscle, we detected cytoplasmic inclusions of GPh in the KO muscle only (Fig. 3A, top row). We performed this analysis with two different GPh antibodies, one provided by Sanger and co-workers (28) (Fig. 3A) and one provided by Carlson (30) (data not shown). Only the Sanger GPh antibody stained the cytoplasmic inclusions; the lack of detection of these inclusions by the Carlson antibody may be due to an

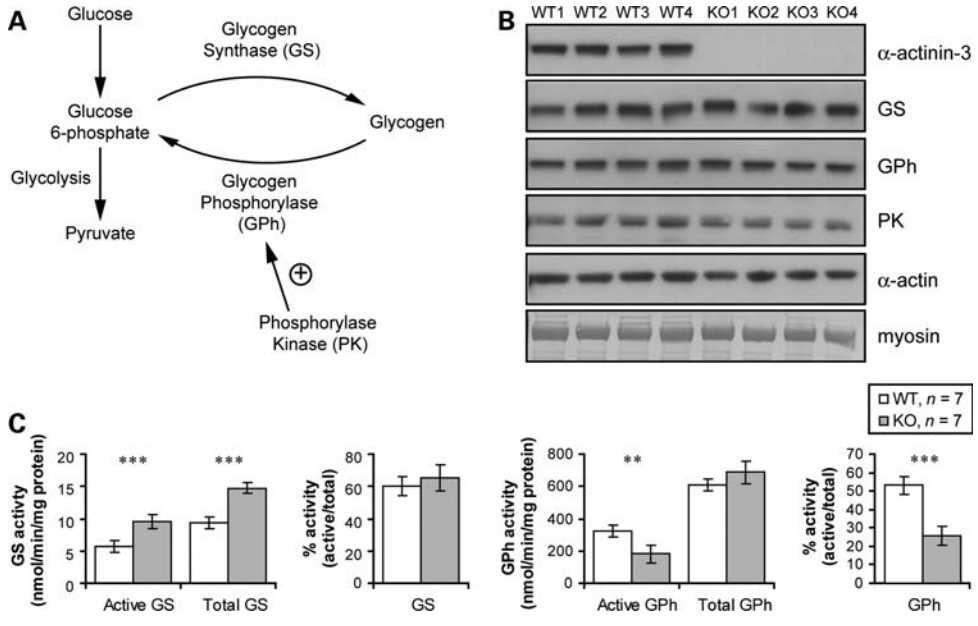

Figure 2. KO mice have lower active GPh. (**A**) Schematic diagram identifying key players in muscle glycogen metabolism. (**B**) There is no detectible difference in the levels of GS, GPh or PK proteins as assessed by western blot. Quadriceps muscle homogenates from four WT and four KO female mice have been compared with antibodies to α-actinin-3, GS, GPh and PK. Samples were loaded for equal myosin and actin content as shown by western blot and Coomassie blue stain, respectively. (**C**) Activities of GS and GPh were assessed in WT and KO quadriceps muscles from 8-week-old male mice. GS and GPh activities were measured in the absence, 'active GS/GPh', and presence, 'total GS/GPh', of 10 mM glucose-6-phosphate or 2.5 mM AMP, respectively, which allosterically activates the inactive portion of the enzyme allowing the total amount of enzyme to be assessed. Mean ± 95% CI, $^{*}P < 0.05$, $^{**}P < 0.01$, $^{***}P < 0.001$.

unusual conformation of GPh in the inclusions resulting in epitope masking. These inclusions are only found within fast-type 2B muscle fibres (as shown by IHC of sequential muscle sections with myosin heavy chain 2B which defines these fibres, Fig. 3A, bottom row), the fibres that normally express α-actinin-3 in WT mice.

In order to develop a more detailed picture of these inclusions, we performed electron microscopy (EM) on WT and KO muscle (Fig. 3B). No gross differences were seen in the sarcomeric structure between KO and WT muscles. However, concentric ring-like structures were seen in all of the KO samples but none of the WT samples. These rings are reminiscent of 'concentric laminated bodies' which can be seen in a variety of muscle disorders and are thought to be of myofibrillar origin (31–33). The concentric ring-like structures in the KO muscle were surrounded by and filled by glycogen particles (Fig. 3B). GPh is known to co-localize with glycogen particles. The nature of the link between the altered regulation of GPh and its localization in cytoplasmic aggregates is unclear; however, the formation of these inclusions in α-actinin-3 deficient muscle provides an additional line of evidence that these two proteins are functionally related.

α-Actinin and glycogen phosphorylase co-localize at the Z-line in KO and WT muscle

To further define the relationship between GPh and α-actinin-3, we examined the localization of these proteins in longitudinal sections of stretched muscle. The use of stretched muscle allows separation between adjacent Z-lines so that localization can be determined with precision. Previous reports have provided contradictory information about the localization of GPh in muscle with studies suggesting that GPh localization is sarcomeric and intermyofibrillar (34), I-band and M-line (35), M-line and Z-line (36) or Z-line (28,37). Our staining suggested Z-line localization of GPh, and partial co-localization between GPh and α-actinin (Fig. 4A). We observed no difference in the localization of GPh in WT and KO muscle, aside from the cytoplasmic inclusions (Fig. 3). The co-localization of these proteins provides further evidence that they are functionally related.

We also examined the localization of PK, the enzyme that phosphorylates and activates GPh. While the total amount of this enzyme was unaltered in KO muscle (Fig. 2B), we hypothesized that differences in the localization of PK in the KO muscle could lead to lower activity of GPh. The PK localization in WT muscle is broadly Z-line, but the PK and α-actinin staining do not co-localize (Fig. 4B). We did not detect any difference in PK localization between WT and KO muscle.

Glycogen phosphorylase displays altered post-translational modification in the absence of α-actinin-3

Global proteomic analysis was performed to detect proteins differentially expressed between WT and KO mouse muscle. α-Actinin-2 was up-regulated in the KO muscle consistent with our previously published western blot analysis (Fig. 5, spot A) (14). Interestingly, three spots within a chain of proteins which were differentially expressed between WT and KO muscle were identified by mass MALDI TOF/TOF mass spectrometry as GPh (Fig. 5, spots C, D and E). This chain of spots is likely to represent post-translationally modified forms of GPh and the particular pattern of spots (increase in pI with no change in size, known as a charge train) is consistent with differentially phosphorylated forms of GPh. Since

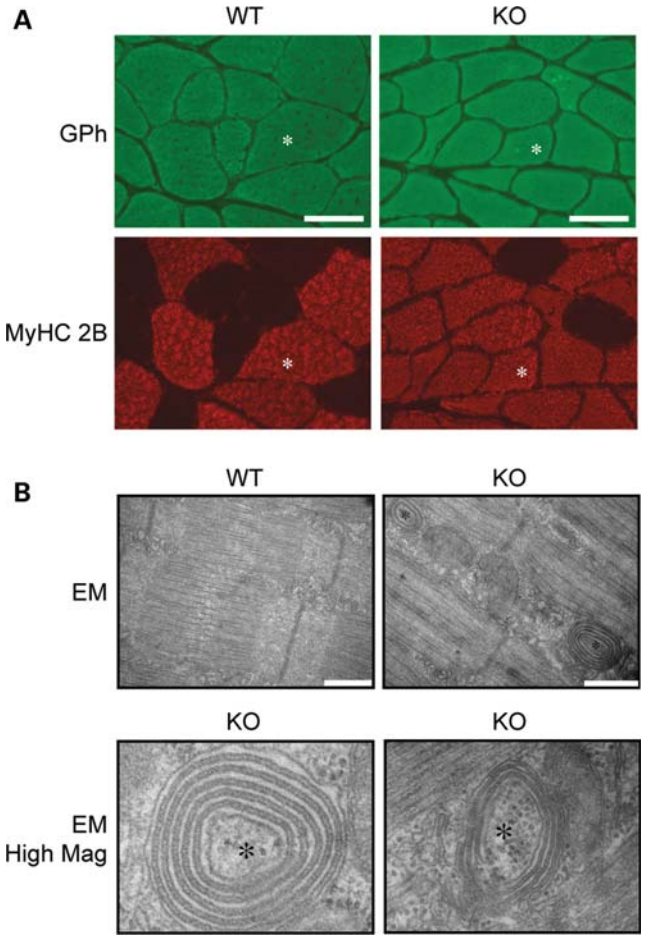

Figure 3. Cytoplasmic inclusions containing GPh are found in KO mouse muscle. (**A**) Representative IHC images of cross-sections of quadriceps muscles from 8-week-old male WT and KO mice. Images were taken on a fluorescent microscope. GPh (top panel) localizes to cytoplasmic inclusions in the KO muscle. A sequential section stained for myosin heavy chain 2B identifies the 2B fast fibres in which α-actinin-3 is expressed in the WT (bottom panel). An asterisk has been used on each of the WT and KO images to allow individual fibres to be readily compared between images. Scale bars are 50 μm wide. (**B**) EM was performed on 50 nm longitudinal sections of vastus lateralis muscles from three WT and three KO 8-week-old female mice. Representative images from 1 WT and KO have been shown with two higher magnification images from the KO below. Concentric ring-like structures are highlighted with black asterisks in the KO panels. Glycogen particles (electron dense circular structures) surround and are contained within the concentric ring-like structures. Scale bars are 500 nm wide.

phosphate groups are negatively charged, if the post-translational modification on GPh is phosphorylation then the spots towards the left of the chain would represent GPh with more phosphate groups. GPh was the first protein shown to be regulated by reversible phosphorylation (38). The phosphorylation of GPh has been extensively studied but to date there has only been one reported phosphorylation site, at serine 14, which is phosphorylated by PK to activate GPh (39). Hence we would expect to see only two post-translational forms of GPh in a 2D gel, one representing the inactive un-phosphorylated form and one representing the active serine 14 phosphorylated form. The identification of seven to eight spots in this GPh charge train suggests that the post-translational modification, and possibly the regulation, of this archetypal phosphoprotein is more complex than has been previously reported. Furthermore, our results suggest that α-actinin-3 is involved in the post-translational modification of GPh.

We used the program FindMod with the list of peptide masses and intensities identified in the above mass spectrometry experiment as the input, but were unable to identify any phosphorylated peptides and, as such, are unable to identify which residues may be being phosphorylated to give rise to the charge train that we observe. Using the protein sequence of mouse GPh, the program NetPhos 2.0 predicts eight high-confidence phosphorylation sites, including the known serine 14 site. The number of sites predicted by NetPhos 2.0 corresponds well to the seven to eight different forms of GPh that we observed in the 2D Gel.

KO muscle is deficient in the spots towards the left of the charge train, likely representing more highly phosphorylated forms of GPh. As the only known phosphorylation of GPh results in an increase in enzyme activity, this lack of phosphorylated GPh may account for the decreased activity of this enzyme in KO muscle.

We have shown here that, in the absence of α-actinin-3, the key glycogen degradation enzyme GPh displays decreased enzymatic activity and is found in cytoplasmic inclusions. GPh and α-actinins co-localize at the muscle Z-line and α-actinin-3 deficiency results in altered post-translational modification of GPh. Added to the fact that GPh has been previously reported to interact with sarcomeric α-actinins, we hypothesized that α-actinin-3 deficiency may alter muscle metabolism and function via direct effects on GPh activity. Such a finding would also suggest that α-actinin-3 plays a role in the regulation of GPh in normal muscle, a function that had not previously been proposed for this structural protein.

Diverse metabolic effects appear concomitantly in the absence of α-actinin-3

We have reported a range of metabolic phenotypic consequences of α-actinin-3 deficiency including decreased GPh activity (this manuscript) and increased activities of glycolytic and mitochondrial enzymes (14). To investigate how these phenotypes are related and which phenotypes are primary versus downstream consequences of α-actinin-3 deficiency, we analysed the metabolic phenotypes of WT and KO muscle during early postnatal development. We compared WT and KO mice at 0, 1, 2 and 4 weeks of age with our existing 8-week-old mouse data to determine the order in which the phenotypic differences between WT and KO mice became apparent. We reasoned that phenotypes that manifest earlier may lie upstream of later phenotypes but that later phenotypes would be unlikely to lie upstream of earlier phenotypes, although we acknowledge that the phenotypes may not be causally related.

We were unable to detect α-actinin-3 expression in newborn mice (Fig. 6A). Expression of α-actinin-3 was barely detectable in muscle at 1 week, but increased over time until the final 8-week time-point. α-Actinin-3 had previously been reported to be expressed in mice from embryonic day 14.5 by IHC, although it was not detectable in skeletal muscle at this time point (3). Thus, it is likely that α-actinin-3 is expressed at birth in mice but at levels undetectable by western blot. The

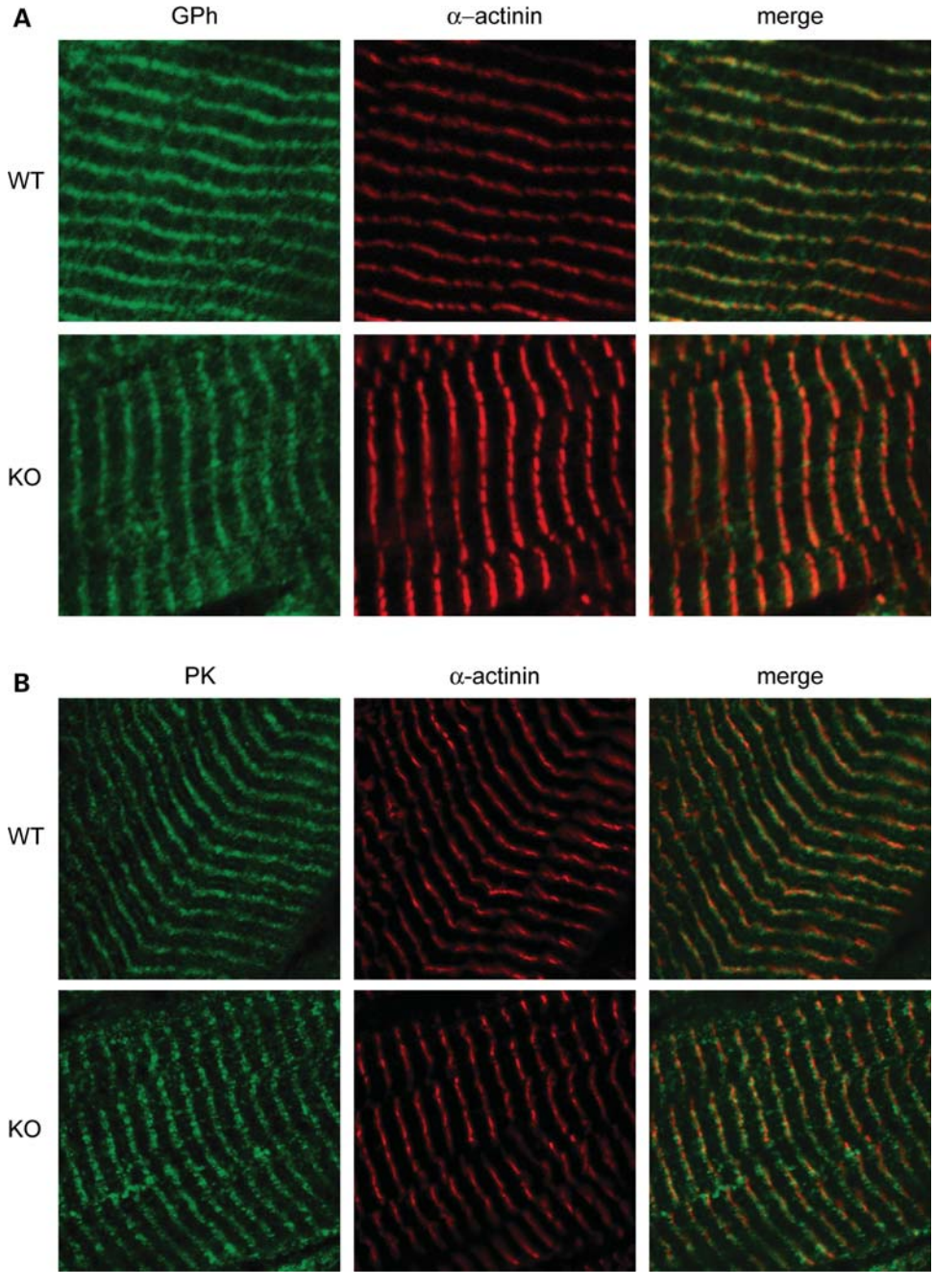

Figure 4. GPh and PK localize to the skeletal muscle Z-line. IHC was performed on single longitudinal sections of stretched vastus lateralis muscles from 8-week-old WT and KO male mice using antibodies to (**A**) GPh (Alexa 488, green) and a mouse α-actinin antibody which recognizes both α-actinin-2 and -3 (Cy3, red, to mark Z-lines) or (**B**) phosphorylase kinase (PK, Alexa 488, green) and α-actinin (Cy3, red as above). Representative images have been shown. Images were taken on a confocal microscope at the same Z-plane and were overlayed in Photoshop to create merge images. Co-localization is seen as yellow in the merge images.

increase in α-actinin-3 expression over time in the WT mice is demonstrated in Figure 6A. As expected, α-actinin-3 expression was not detected in KO muscle at any age.

Increase in glycogen content and reduction in the activity of GPh (Supplementary Material, Fig. S3, summarized in Fig. 6B), and increase in the activity of glycolytic and mitochondrial enzymes (Supplementary Material, Fig. S4, summarized in Fig. 6B) were only apparent in the KO muscle from 4 weeks of age. The concomitant appearance of these two phenotypes is consistent with the hypothesis that changes in GPh metabolism are related to the other metabolic effects seen in KO muscle.

Differentiated primary mouse myoblasts from KO mice have altered calcium handling

It has previously been reported that GPh-a (the serine-14 phosphorylated, active form of GPh) acts as a negative

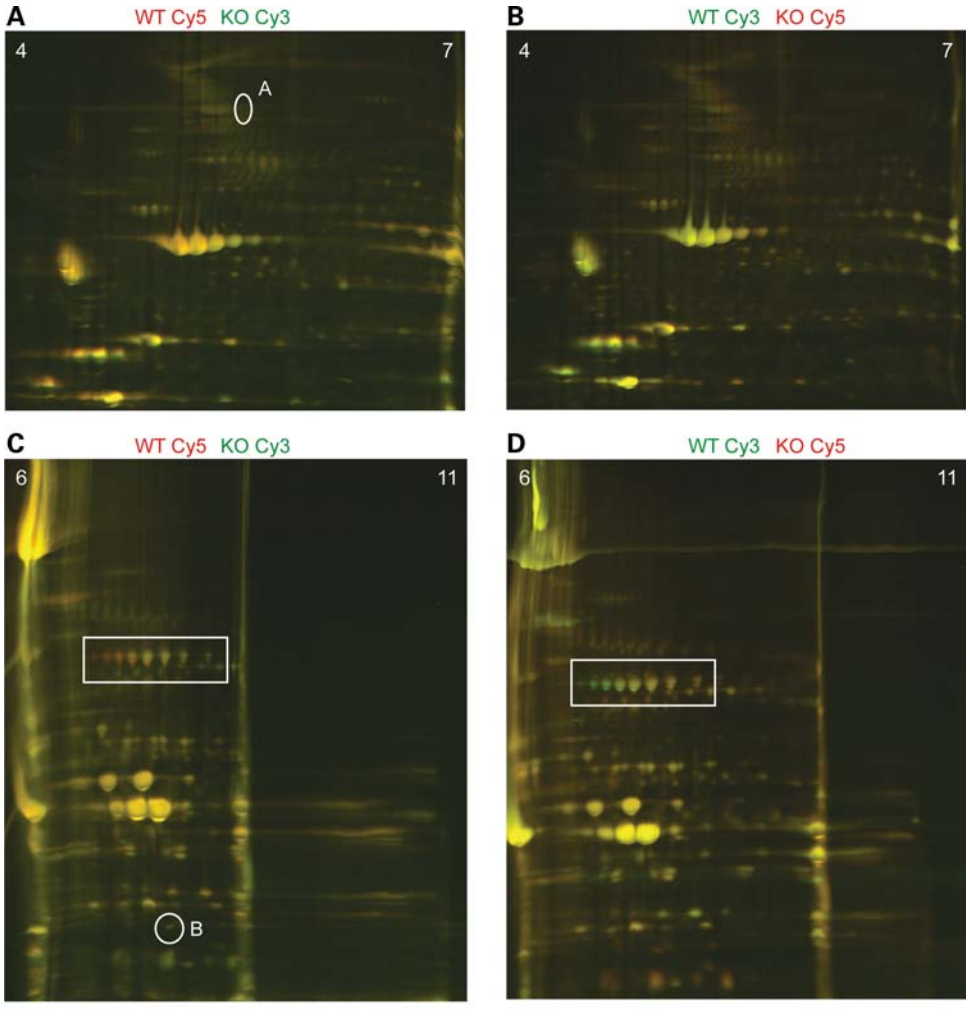

F

Spot	Fold Difference *	Accession	Mass Spec ID	Mass	Theortical pI
A	2.145	gi|77736221	actinin alpha 2 [Mus musculus]	103853	5.31
B	2.913	gi|6753530	crystallin, alpha B [Mus musculus]	20056	6.76
C	-3.043	gi|6755256	muscle glycogen phosphorylase [Mus musculus]	97225	6.65
D	-2.422	gi|6755256	muscle glycogen phosphorylase [Mus musculus]	97225	6.65
E	1.169	gi|6755256	muscle glycogen phosphorylase [Mus musculus]	97225	6.65

* positive fold difference indicates protein is more abundant in KO sample

Figure 5. GPh is differentially post-translationally modified in the KO mouse. (**A**–**D**) A proteomic analysis was performed on TA muscle extracts from four WT and four KO 8-week-old male mice. The composite WT sample was labelled with a Cy5 DIGE label and the composite KO sample was labelled with a Cy3 DIGE label (A and C). The dye-swap experiment was also run (B and D). Second dimension SDS–PAGE gels from isoelectric focussing strips [pI 4–7 in (A) and (B) and pI 6–11 in (C) and (D)] are shown. Yellow spots indicate proteins which are equally expressed in the WT and KO. Green spots in (A) and (B) and red spots in (C) and (D) indicate proteins that are more abundant in the KO. (**E**) Area of gels C and D (white boxes) have been enlarged to allow a series of spots to be examined. These spots are differentially expressed in the KO and WT with lower levels of the more acidic (left hand side of the gels) spots in the KO sample. (**F**) A number of spots were excised from the gel and the identities of these proteins were determined by MALDI TOF/TOF mass spectrometry. The excised spots have been demarcated by white circles in the gel images and the identities of the proteins have been shown. Three spots in the chain of spots in (E) were identified as muscle GPh with two of the more acidic spots (C and D) being markedly reduced in the KO muscle.

regulator of sarcoplasmic reticulum calcium release in muscle (40). We have previously demonstrated that isolated muscle fibres from the *Actn3* KO mice have altered contractile properties: KO fibres have longer half-relaxation times, generate less force and have enhanced recovery following muscle fatigue when compared with WT fibres (15). Since muscle contraction and relaxation are greatly reliant on the rapidity of calcium release and uptake from the sarcoplasmic reticulum, we were interested in whether the changes in GPh activity reported here could underlie the

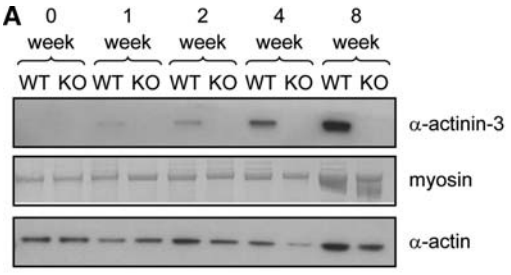

B

Effects in KO mice as compared to WT controls	Mouse Age				
	0 week	1 week	2 week	4 week	8 week
Lower activity of GPh	×	×	×	✓	✓
Higher muscle glycogen content	×	×	×	✓	✓
Higher enzyme activities of HK and mitochondrial enzymes CS, SDH and BHAD	×	×	×	✓	✓

Figure 6. The onset of metabolic phenotypes in the KO mouse over time. (**A**) Western blots were performed using extracts from 0-, 1-, 2-, 4- and 8-week-old WT and KO mouse muscles. Levels α-actinin-3 as detected by specific antibody was examined over time. Samples were loaded for equal myosin and actin content as shown by western blot and Coomassie blue stain, respectively. (**B**) Summary of the onset of various metabolic consequences of α-actinin-3 deficiency over time (from Supplementary Material, Figs S3–S4).

differences in contractile properties seen between our KO and WT mice.

We assessed intracellular calcium transients in differentiated primary WT and KO cultured myotubes; WT myotubes express α-actinin-3, and study of myotubes allows us to determine properties intrinsic to the muscle itself, in isolation from other variables that may influence results *in vivo*. We loaded the myotubes with Fura-2AM, a dye that alters its excitation wavelength when bound to calcium. Upon electrical stimulation, calcium is released into the cytoplasm through the activation of the dihydropyridine receptor and the opening of the ryanodine receptors in the sarcoplasmic reticulum is bound briefly by Fura-2AM, then rapidly dissociates from the dye as calcium is re-sequestered by the sarcoplasmic reticulum or becomes bound to calcium binding proteins such as calmodulin in calcium signalling, or troponins to initiate muscle contraction. Intracellular calcium transients can therefore be determined from the ratio of bound versus unbound Fura-2AM to calcium by measuring its emission spectra at different excitation wavelengths.

Comparison of mature, contracting WT and KO myotube cultures showed significant differences in calcium handling between the different genotypes (Fig. 7). KO myotubes have significantly higher peak height ratio values, suggesting greater calcium release in the KO upon electrical stimulation, although the percentage increase in intracellular free calcium between WT and KO is not significantly different. KO myotubes also showed significantly higher departure and return velocities, indicating that calcium in KO cells is released and sequestered more rapidly than in WT cells.

DISCUSSION

Although the sarcomeric α-actinins have been considered to be primarily structural proteins, the dominant phenotype in the *Actn3* KO mouse is an alteration in the metabolic profile of fast glycolytic muscle fibres, with normal sarcomere formation (14,15). The switch towards aerobic metabolism in α-actinin-3 deficient muscle provides a logical explanation for the reported associations between *ACTN3* genotype and human skeletal muscle performance. However, the link between α-actinin-3 deficiency and its metabolic and functional consequences has not yet been defined.

Due to the previously reported interaction of GPh and sarcomeric α-actinins, we investigated glycogen content in our KO muscles and show that the levels of glycogen are significantly higher in KO than WT muscles by several methods. The glycogen content was also shown to be higher in 577XX (α-actinin-3 deficient) humans when compared with 577RX humans. An increase in the activity of GS or a decrease in the activity of GPh, the key regulatory enzymes in glycogen synthesis and glycogen degradation, respectively, could account for this finding. Here we demonstrate that there is a marked (∼50%) decrease in the activity of GPh in muscle in α-actinin-3 deficient mice, as well as an increase in the total amount (but not percentage activity) of GS, both of which are likely to contribute to increased glycogen content. GPh and α-actinins co-localize in skeletal muscle and cytoplasmic inclusions contain GPh form in α-actinin-3 deficient muscle. The glycogen pathway is tightly controlled and it is thus possible that the up-regulation of GS is a downstream compensatory consequence of decreased GPh activity. GPh is regulated by reversible phosphorylation (38), and phosphorylation by PK leads to the activation of GPh. We demonstrate differences in the levels of putative phosphorylation in WT and KO mice that correspond to reduction in the activity of GPh associated with α-actinin-3 deficiency. Taken together, these lines of evidence strongly suggest that α-actinin-3 plays a role in the post-translational regulation of GPh.

Regardless of the mechanism by which GPh activity is altered in α-actinin-3 deficient muscle, a reduced capacity to break down glycogen for energy would be likely to have direct effects on muscle function. α-Actinin-3 deficiency is detrimental to sprint and power activity in human athlete and non-athlete populations (4). We demonstrate that the lower GPh activity and higher muscle glycogen content occur simultaneously with the onset of higher activity of glycolytic and mitochondrial enzymes in α-actinin-3 deficient mouse muscle in a developmental time course. A reduced ability to access muscle glycogen would be disadvantageous to sprint athletes, who rely on endogenous fuels such as muscle glycogen to rapidly produce energy for contraction. Reduced availability of glucose may, in turn, result in a compensatory shift towards aerobic metabolism, as observed in KO mice. Such changes could be advantageous to endurance athletes, allowing them to preserve muscle glycogen and preferentially use other fuels such as fatty acids for energy generation.

Interestingly, the decrease in GPh activity caused by α-actinin-3 deficiency may provide a mechanism for changes in the contractile properties, in addition to metabolic differences, seen in *Actn3* KO mice. *Actn3* KO muscles display longer twitch half-relaxation times, lower force generation and greater fatigue resistance than WT muscles (15). Serine-14-phosphorylated GPh, but not the un-phosphorylated

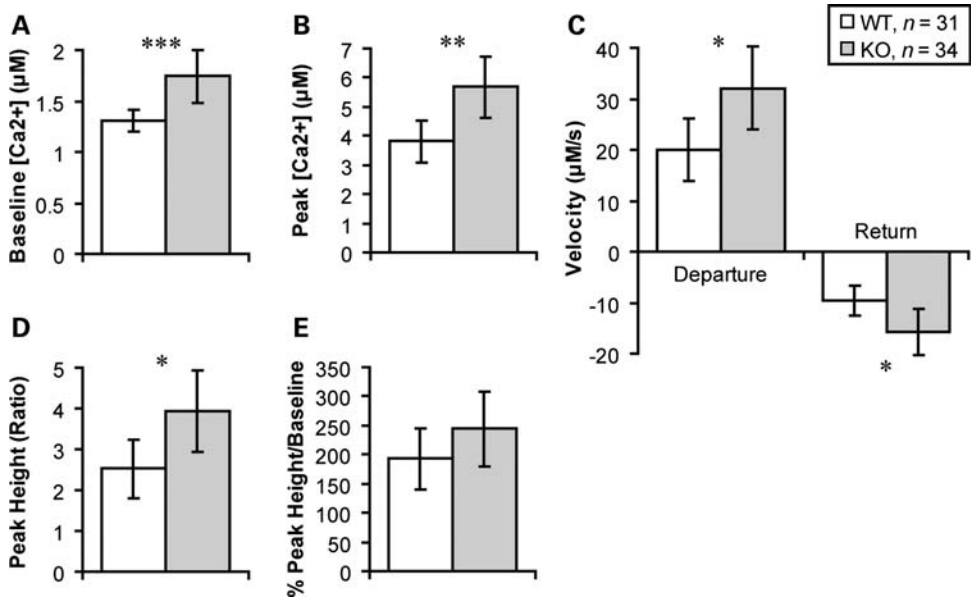

Figure 7. KO myotubes have altered calcium dynamics. KO myotubes showed higher free intracellular calcium levels at baseline (**A**), as well as greater calcium release in response to a single 30 V stimulus (1 ms, 0.33 Hz), as shown by higher peak calcium (**B**) and peak height (**D**), though percentage increase was not significantly different (**E**). KO myotubes also had a faster departure and return velocity than WT myotubes, suggesting faster calcium release and uptake in cells in the absence of α-actinin-3 (**C**). Myotubes were pooled from post-differentiation days 4, 5 and 6. Only contracting myotubes were included in this study. Mean ± 95% CI, $^{*}P < 0.05$, $^{**}P < 0.01$, $^{***}P < 0.001$.

form, has been shown to be a negative regulator of calcium release from the sarcoplasmic reticulum, a critical step in the regulation of muscle contraction mediated by ryanodine receptors (40). We have demonstrated that GPh activity is lower in *Actn3* KO muscles and that this is likely due to lower levels of GPh phosphorylation; so decreased GPh activity in KO muscles may result in reduced inhibition of the ryanodine receptors leading to greater rates of calcium release. We tested this hypothesis, and indeed observe changes in calcium regulation in isolated myotubes that likely contribute to the changes in contractile properties seen in α-actinin-3 deficient muscle.

We propose the following working model: α-actinin-3 deficiency results in altered regulation of GPh, leading to an increase in muscle glycogen content, and decreasing the capacity of muscle to use glycogen as a fuel. This, in turn, results in a switch in preferred fuel source, with a decrease in anaerobic metabolism and an increase in oxidative metabolism as seen in KO mice. The alterations in muscle contractile properties could be a direct consequence of the reduction in active GPh altering calcium regulation, could be due to the switch towards aerobic metabolism or, more likely, represent a combination of the two processes.

Here we present the first direct evidence, to our knowledge, for a role of α-actinin-3 in the regulation of glycogen metabolism and provide biochemical insight into how a common human null polymorphism in *ACTN3* in humans leads to changes in muscle metabolism and function. The X allele has undergone positive selection during recent human evolution (14), suggesting that the effects of α-actinin-3 deficiency on muscle metabolism and muscle contraction provided a fitness advantage in response to environmental stressors. For example, it is possible that a switch from glycogen to fatty acids as a preferred fuel source in skeletal muscle is protective during times of famine. As a consequence of this positive selection, α-actinin-3 is deficient in ∼16% of modern humans worldwide, and the study of this protein is relevant to the understanding of normal human variation in skeletal muscle performance in health and disease, as well as adaptation to alterations in the environment and diet.

MATERIALS AND METHODS

Animals

This study was approved by our local Animal Care and Ethics Committee. All tests were performed on N4 mice of 129 genetic background, as described previously (14). All mice were fed food and water *ad libitum*, and were maintained on a 12:12 h cycle of light and dark.

Human samples

This study was approved by the ethics committees of The Children's Hospital at Westmead, Sydney, Australia, and informed consent for tissue and DNA samples was obtained from all participating individuals.

Tissue collection

Mice were euthanized immediately prior to muscle collection. Eight- and 4-week-old mice were euthanized by cervical dislocation, whereas newborn (0 week), 1- and 2-week-old mice were euthanized by decapitation. Individual muscles were harvested from the 8- and 4-week-old mice. For newborn, 1- and 2-week-old mice, the upper hind limb (the

section between the hip and knee, mainly quadriceps muscle) was removed and skinned. Muscles were immediately snap-frozen in liquid nitrogen for metabolic enzyme analysis or covered in cryo-preservation medium (Tissue-Tek) and frozen in partly thawed isopentane. The vastus lateralis muscle was dissected away from the other quadriceps muscles and stretched longitudinally, clamped and fixed in 3% paraformaldehyde for 10 min before clamps were released and muscle was coated in cryo-preservation medium and frozen. Tissue was stored in liquid nitrogen.

Human quadriceps muscle biopsies were obtained from patients undergoing testing for malignant hyperthermia and were all from individuals who tested negative and thus were control individuals. Biopsies were covered in cryo-preservation medium (Tissue-Tek) and frozen in partly thawed isopentane. Tissue was stored in liquid nitrogen.

Histochemistry

Transverse 8 μm sections were cut from the mid-section of frozen quadriceps muscles. PAS stains were performed using standard protocols (see Supplementary Methods for details).

Antibodies

An antibody (Ab) to α-actinin-3 was a gift from A. Beggs (Children's Hospital Boston) and α-actinin-3 rabbit Ab 5B3 was used at 1:12000 for WB. A mouse sarcomeric α-actinin (Sigma A5044) Ab (recognizing both α-actinin-2 and -3) was used at 1:400 for IHC. An antibody to α-sarcomeric actin (5C5, mouse Ab, Sigma, WB 1:2000) was used. Two different antibodies to muscle GPh (PYGM) were used; the rabbit amorphin Ab (amorphin is GPh) provided by J. Sanger (University of Pennsylvania School of Medicine) (28) for IHC at 1:100 and a rabbit GPh Ab provided by G. Carlson (University of Kansas Medical Centre) and A. DePaoli-Roach (Indiana University School of Medicine) (30) at 1:50 for IHC and 1:5000 for WB. A rabbit Ab to GS (no. 3893, Cell Signalling) was used for WB at 1:1000. Two different antibodies to a subunit of PK (PHKA1) were used. A rabbit Sigma PHKA1 Ab was used at 1:50 for IHC. A mouse Abnova PHKA1 Ab was used at 1:2000 for WB. For details of immunoblotting and IHC methods, please see Supplementary Methods.

Electron microscopy (EM) and tomography

EM blocks were prepared from spinalis thoracis muscles from WT and KO 8-week-old male mice and vastus lateralis muscles from WT and KO 8-week-old female mice. These muscles were cut into strips in glutaraldehyde-based fixative and then minced into cubes with the smallest dimension being less than 1 mm. Processing was done using standard methods. For electron tomography, 300 nm sections of vastus lateralis muscles were stained and labelled with 15 nm gold as a fiducial marker. Dual axis tilt series from +60 to −60 degrees were obtained in a Tecnai F30 300 kV TEM using the SerialEM software package. An estimate of glycogen content was obtained by point counting using standard stereological techniques. Points over glycogen particles were related to the cytoplasmic volume on at least 10 images from each of the tomograms.

Total glycogen assays

Total glycogen assays were performed essentially as previously described (41). For a detailed description of the method, see Supplementary Methods.

Glycogen synthase and glycogen phosphorylase assays

GS and GPh assays were performed using modifications of existing prototols (42,43). For a detailed description, see Supplementary Methods.

Enzyme assays

The activities of the enzymes hexokinase (HK, EC 2.7.1.1), citrate synthase (EC 4.1.3.7), lactate dehydrogenase (EC 1.1.1.27), 3-hydroxyacyl-CoA dehydrogenase (BHAD, EC 1.1.1.35), phosphofructokinase (2.7.1.11) and succinate dehydrogenase (SDH, 1.3.5.1) were determined spectrophotometrically in homogenized muscle extracts from WT and KO mice using methods described previously (15). Assays were performed at 30°C in duplicate and values were averaged. Activities were corrected for total protein content as measured using the BioRad Protein Assay (500-0006), according to the manufacturer's instructions, for BSA standards and extracts in duplicate. The mg protein in each extract was used to convert the activities of each enzyme (mU) to specific activities (mU/mg or nmol/min/mg protein).

Proteomic analysis

A proteomic analysis was performed on tibialis anterior muscles from 8-week-old male WT and KO mice by the Australian Proteome Analysis Facility using standard protocols. For a detailed description, see Supplementary Methods.

Measurement of intracellular Ca^{2+} transients

For a detailed description of the establishment of the primary mouse myoblast cell lines, see Supplementary Methods. To determine baseline differences in calcium handling, WT and KO myotubes were plated on glass coverslips and differentiated in low serum media (1:1 DMEM:HAMS F12, 3% horse serum, 1% Insulin-Selenium-Transferrin (Invitrogen), 10 mg/ml gentamycin). From differentiation days 4 to 7, coverslips were rinsed with standard external 1.8 Ca^{2+} solution (130 mM NaCl, 5.4 mM KCl, 1.8 mM $CaCl_2$, 0.8 mM $MgCl_2$, 10 mM HEPES, 5.6 mM d-glucose, pH 7.4 with NaOH) and incubated: first for 40 min at room temperature, then for 5 min at 37°C in the same solution supplemented with 3 μM (final concentration) fura-2 AM (Invitrogen, Australia). After fura-2 loading, cells were again washed with 1.8 Ca^{2+} solution, and the coverslip transferred to a perfusion chamber (CSTRGPKG-Culture/Stim remove glass PKG; SDR Clinical technology, Australia) filled with 1.8 Ca^{2+} solution. Fura-2-loaded cells were excited at 340 and 380 nm with a IonOptix hyperswitch light source (the excitation wavelength was

rapidly switched at a rate of 250 ratios/s), and emission fluorescence was monitored at 510 nm using an Intensified MyoCam CCD video camera (IonOptix, USA) attached to a Nikon TE2000-U microscope (×40 oil immersion fluorescence objective) (Coherent Scientifique, Australia). Myotubes were field stimulated using platinum electrodes (MyoPacer field stimulator, IonOptix, USA). The variation of fluorescence was recorded and analysed with the IonOptix Digital Image Acquisition Software (IonOptix, USA). Statistical analysis was performed with Origin 5.0 software (OriginLab, Northampton, MA, USA).

Statistics

All comparisons reported in this study involved small sample sizes to which standard tests for normality could not be applied. As such, all comparisons of means were performed using the non-parametric Mann–Whitney *U* test. All histograms show mean values, with error bars indicating 95% confidence intervals (95% CI) unless otherwise stated.

SUPPLEMENTARY MATERIAL

Supplementary Material is available at *HMG* online.

ACKNOWLEDGEMENTS

Valentina Valova and Phil Robinson from Children's Medical Research Institute, Australia, for invaluable help with interpretation of mass spec data; Neil Street from the Children's Hospital at Westmead for providing the human muscle samples; Gerald Carlson, Anna dePaoli-Roach Joseph Sanger and Alan Beggs for providing antibodies; Ross Boadle, Emma Kettle, Marko Nykanen and Edna Hardeman for assistance with EM sample preparation and analysis; the Australian Proteome Analysis Facility for the proteomic analysis; Nicole Schieber for technical help.

Conflict of Interest statement. None declared.

FUNDING

This project was supported by a grant (512254) from the Australian National Health and Medical Research Council (NHMRC). D.G.M. and J.T.S. were supported by Australian Postgraduate Awards. N.T. and G.J.C. were supported by a Career Development Award and a Senior Research Fellowship from the NHMRC, respectively.

REFERENCES

1. Beggs, A.H., Byers, T.J., Knoll, J.H., Boyce, F.M., Bruns, G.A. and Kunkel, L.M. (1992) Cloning and characterization of two human skeletal muscle alpha-actinin genes located on chromosomes 1 and 11. *J. Biol. Chem.*, **267**, 9281–9288.
2. North, K.N., Yang, N., Wattanasirichaigoon, D., Mills, M., Easteal, S. and Beggs, A.H. (1999) A common nonsense mutation results in alpha-actinin-3 deficiency in the general population. *Nat. Genet.*, **21**, 353–354.
3. Mills, M., Yang, N., Weinberger, R., Vander Woude, D.L., Beggs, A.H., Easteal, S. and North, K. (2001) Differential expression of the actin-binding proteins, alpha-actinin-2 and -3, in different species: implications for the evolution of functional redundancy. *Hum. Mol. Genet.*, **10**, 1335–1346.
4. Yang, N., MacArthur, D.G., Gulbin, J.P., Hahn, A.G., Beggs, A.H., Easteal, S. and North, K. (2003) ACTN3 genotype is associated with human elite athletic performance. *Am. J. Hum. Genet.*, **73**, 627–631.
5. Santiago, C., Gonzalez-Freire, M., Serratosa, L., Morate, F.J., Meyer, T., Gomez-Gallego, F. and Lucia, A. (2008) ACTN3 genotype in professional soccer players. *Br. J. Sports Med.*, **42**, 71–73.
6. Druzhevskaya, A.M., Ahmetov, I.I., Astratenkova, I.V. and Rogozkin, V.A. (2008) Association of the ACTN3 R577X polymorphism with power athlete status in Russians. *Eur. J. Appl. Physiol.*, **103**, 631–634.
7. Niemi, A.K. and Majamaa, K. (2005) Mitochondrial DNA and ACTN3 genotypes in Finnish elite endurance and sprint athletes. *Eur. J. Hum. Genet.*, **13**, 965–969.
8. Papadimitriou, I.D., Papadopoulos, C., Kouvatsi, A. and Triantaphyllidis, C. (2008) The ACTN3 gene in elite Greek track and field athletes. *Int. J. Sports Med.*, **29**, 352–355.
9. Roth, S.M., Walsh, S., Liu, D., Metter, E.J., Ferrucci, L. and Hurley, B.F. (2008) The ACTN3 R577X nonsense allele is under-represented in elite-level strength athletes. *Eur. J. Hum. Genet.*, **16**, 391–394.
10. Eynon, N., Duarte, J.A., Oliveira, J., Sagiv, M., Yamin, C., Meckel, Y., Sagiv, M. and Goldhammer, E. (2009) ACTN3 R577X polymorphism and Israeli top-level athletes. *Int. J. Sports Med.*, **30**, 695–698.
11. Clarkson, P.M., Devaney, J.M., Gordish-Dressman, H., Thompson, P.D., Hubal, M.J., Urso, M., Price, T.B., Angelopoulos, T.J., Gordon, P.M., Moyna, N.M. *et al.* (2005) ACTN3 genotype is associated with increases in muscle strength in response to resistance training in women. *J. Appl. Physiol.*, **99**, 154–163.
12. Moran, C.N., Yang, N., Bailey, M.E., Tsiokanos, A., Jamurtas, A., MacArthur, D.G., North, K., Pitsiladis, Y.P. and Wilson, R.H. (2007) Association analysis of the ACTN3 R577X polymorphism and complex quantitative body composition and performance phenotypes in adolescent Greeks. *Eur. J. Hum. Genet.*, **15**, 88–93.
13. North, K.N. and Beggs, A.H. (1996) Deficiency of a skeletal muscle isoform of alpha-actinin (alpha-actinin-3) in merosin-positive congenital muscular dystrophy. *Neuromuscul. Disord.*, **6**, 229–235.
14. MacArthur, D.G., Seto, J.T., Raftery, J.M., Quinlan, K.G., Huttley, G.A., Hook, J.W., Lemckert, F.A., Kee, A.J., Edwards, M.R., Berman, Y. *et al.* (2007) Loss of ACTN3 gene function alters mouse muscle metabolism and shows evidence of positive selection in humans. *Nat. Genet.*, **39**, 1261–1265.
15. MacArthur, D.G., Seto, J.T., Chan, S., Quinlan, K.G., Raftery, J.M., Turner, N., Nicholson, M.D., Kee, A.J., Hardeman, E.C., Gunning, P.W. *et al.* (2008) An Actn3 knockout mouse provides mechanistic insights into the association between alpha-actinin-3 deficiency and human athletic performance. *Hum. Mol. Genet.*, **17**, 1076–1086.
16. Salmikangas, P., Mykkanen, O.M., Gronholm, M., Heiska, L., Kere, J. and Carpen, O. (1999) Myotilin, a novel sarcomeric protein with two Ig-like domains, is encoded by a candidate gene for limb-girdle muscular dystrophy. *Hum. Mol. Genet.*, **8**, 1329–1336.
17. Hance, J.E., Fu, S.Y., Watkins, S.C., Beggs, A.H. and Michalak, M. (1999) Alpha-actinin-2 is a new component of the dystrophin–glycoprotein complex. *Arch. Biochem. Biophys.*, **365**, 216–222.
18. Xia, H., Winokur, S.T., Kuo, W.L., Altherr, M.R. and Bredt, D.S. (1997) Actinin-associated LIM protein: identification of a domain interaction between PDZ and spectrin-like repeat motifs. *J. Cell Biol.*, **139**, 507–515.
19. Klaavuniemi, T., Kelloniemi, A. and Ylanne, J. (2004) The ZASP-like motif in actinin-associated LIM protein is required for interaction with the alpha-actinin rod and for targeting to the muscle Z-line. *J. Biol. Chem.*, **279**, 26402–26410.
20. Lu, S., Carroll, S.L., Herrera, A.H., Ozanne, B. and Horowits, R. (2003) New N-RAP-binding partners alpha-actinin, filamin and Krp1 detected by yeast two-hybrid screening: implications for myofibril assembly. *J. Cell Sci.*, **116**, 2169–2178.
21. Niederlander, N., Fayein, N.A., Auffray, C. and Pomies, P. (2004) Characterization of a new human isoform of the enigma homolog family specifically expressed in skeletal muscle. *Biochem. Biophys. Res. Commun.*, **325**, 1304–1311.
22. Sorimachi, H., Freiburg, A., Kolmerer, B., Ishiura, S., Stier, G., Gregorio, C.C., Labeit, D., Linke, W.A., Suzuki, K. and Labeit, S. (1997) Tissue-specific expression and alpha-actinin binding properties of the

Z-disc titin: implications for the nature of vertebrate Z-discs. *J. Mol. Biol.*, **270**, 688–695.
23. Faulkner, G., Pallavicini, A., Formentin, E., Comelli, A., Ievolella, C., Trevisan, S., Bortoletto, G., Scannapieco, P., Salamon, M., Mouly, V. *et al.* (1999) ZASP: a new Z-band alternatively spliced PDZ-motif protein. *J. Cell. Biol.*, **146**, 465–475.
24. Frey, N. and Olson, E.N. (2002) Calsarcin-3, a novel skeletal muscle-specific member of the calsarcin family, interacts with multiple Z-disc proteins. *J. Biol. Chem.*, **277**, 13998–14004.
25. Mukai, H., Toshimori, M., Shibata, H., Takanaga, H., Kitagawa, M., Miyahara, M., Shimakawa, M. and Ono, Y. (1997) Interaction of PKN with alpha-actinin. *J. Biol. Chem.*, **272**, 4740–4746.
26. Maruoka, N.D., Steele, D.F., Au, B.P., Dan, P., Zhang, X., Moore, E.D. and Fedida, D. (2000) Alpha-actinin-2 couples to cardiac Kv1.5 channels, regulating current density and channel localization in HEK cells. *FEBS Lett.*, **473**, 188–194.
27. Cukovic, D., Lu, G.W., Wible, B., Steele, D.F. and Fedida, D. (2001) A discrete amino terminal domain of Kv1.5 and Kv1.4 potassium channels interacts with the spectrin repeats of alpha-actinin-2. *FEBS Lett.*, **498**, 87–92.
28. Chowrashi, P., Mittal, B., Sanger, J.M. and Sanger, J.W. (2002) Amorphin is phosphorylase; phosphorylase is an alpha-actinin-binding protein. *Cell Motil. Cytoskeleton*, **53**, 125–135.
29. Gizak, A., Rakus, D. and Dzugaj, A. (2003) Immunohistochemical localization of human fructose-1,6-bisphosphatase in subcellular structures of myocytes. *Histol. Histopathol.*, **18**, 135–142.
30. Prats, C., Cadefau, J.A., Cusso, R., Qvortrup, K., Nielsen, J.N., Wojtaszewski, J.F., Hardie, D.G., Stewart, G., Hansen, B.F. and Ploug, T. (2005) Phosphorylation-dependent translocation of glycogen synthase to a novel structure during glycogen resynthesis. *J. Biol. Chem.*, **280**, 23165–23172.
31. Dubowitz, V. and Sewry, C.A. (2007) *Muscle Biopsy—A Practical Approach*, 3rd edn. Saunders Elsevier.
32. Yarom, R. and Shapira, Y. (1981) Concentric laminated bodies. *Muscle Nerve*, **4**, 259–260.
33. Engel, A.G. and Franzini-Armstrong, C. (2004) *Myology*, 3rd edn. McGraw-Hill, New York.
34. Dvorak, H.F. and Cohen, R.B. (1965) Localization of skeletal muscle phosphorylase using a fluorescent antibody technique and its correlation with histochemical observations. *J. Histochem. Cytochem.*, **13**, 454–460.
35. Heizmann, C.W. and Eppenberger, H.M. (1978) Isolation and characterization of glycogen phosphorylase b from chicken breast muscle: comparison with a protein extracted from the M. line. *J. Biol. Chem.*, **253**, 270–277.
36. Maruyama, K., Kuroda, M. and Nonomura, Y. (1985) Association of chicken pectoralis muscle phosphorylase with the Z-line and the M-line of myofibrils: comparison with 'amorphin', the amorphous component of the Z-line. *Biochim. Biophys. Acta*, **829**, 229–237.
37. Trinick, J. and Lowey, S. (1977) M-protein from chicken pectoralis muscle: isolation and characterization. *J. Mol. Biol.*, **113**, 343–368.
38. Fischer, E.H. and Krebs, E.G. (1955) Conversion of phosphorylase b to phosphorylase a in muscle extracts. *J. Biol. Chem.*, **216**, 121–132.
39. Titani, K., Cohen, P., Walsh, K.A. and Neurath, H. (1975) Amino-terminal sequence of rabbit muscle phosphorylase. *FEBS Lett.*, **55**, 120–123.
40. Hirata, Y., Atsumi, M., Ohizumi, Y. and Nakahata, N. (2003) Mastoparan binds to glycogen phosphorylase to regulate sarcoplasmic reticular Ca2+ release in skeletal muscle. *Biochem. J.*, **371**, 81–88.
41. Johnson, J.A. and Fusaro, R.M. (1966) The quantitative enzymic determination of animal liver glycogen. *Anal. Biochem.*, **15**, 140–149.
42. Thomas, J.A., Schlender, K.K. and Larner, J. (1968) A rapid filter paper assay for UDPglucose-glycogen glucosyltransferase, including an improved biosynthesis of UDP-14C-glucose. *Anal. Biochem.*, **25**, 486–499.
43. Gilboe, D.P., Larson, K.L. and Nuttall, F.Q. (1972) Radioactive method for the assay of glycogen phosphorylases. *Anal. Biochem.*, **47**, 20–27.